Journal of Engineering Research and Applied Science
Available at www.journaleras.com
Volume 7 (2), December 2018, pp 869-877
ISSN 2147-3471 © 2018

Removal of dimozol red dye by adsorption onto chitosan/marble powder composite: adsorption kinetics and isotherms

D. Akin Sahbaz[1], S. Dandil[2], C. Acikgoz[2,a]

[1]1Afyon Kocatepe University, Department of Chemical Engineering, Afyon,Turkey.
[2]Bilecik Seyh Edebali University, Department of Chemical Engineering, Bilecik, Turkey.

Accepted 25 August 2018

Abstract
In this study, chitosan (C)/marble powder (M) composites were used as an adsorbent for the removal of Dimozol Red Dye from aqueous solution. Chitosan (C)/marble powder (M) composites with different weight ratio percentage (C100M0, C70M30, C50M50 and C30M70) were prepared with marble powder and chitosan. Batch studies were carried out to address various experimental parameters such as contact time (0-72 hours), pH (3-11), adsorbent dosage (0.2-2.0 g/L) and initial dye concentration (40-100 mg/L). Equilibrium isotherms were analyzed by Langmuir, Freundlich, Temkin and Dublin-Radushkevich isotherm equations using correlation cooefficients and the results were best represented by Freundlich isotherm model. And also, adsorption kinetic was performed using the pseudo-first-order, the pseudo-second-order and intra-particle diffusion kinetic models. The adsorption kinetics well fitted with a pseudo-second-order kinetic model.

Keywords: Adsorption; adsorption isotherms; adsorption kinetics; chitosan; dimozol red.

1. Introduction

Synthetic dyes are widely used as coloring agents in several industries like textile, printing, leather, food and cosmetics. Some of these dyes are highly toxic, carcinogenic and/or mutagenic in nature and thereby pose threats to human and other living organisms in the environment. The main methods of removing dyes from industrial effluents are biodegradation [1], electrocoagulation [2], chemical coagulation [3], oxidation [4] and adsorption [5]. Because of the simplicity in its design and operation adsorption has been found to be an effective method with its ability to adsorb a broad range of pollutants; and fast processing [6].

Adsorbent, chemical structure of dye and process conditions has significant effects on performance of adsorption processes can vary all process kinetics and eqilibrium. Activated carbon is known as an efficient adsorbent with its high surface area and efficiency, but its high cost limits its wide application. In recent years, researchers have been developed several new effective and cheaper adsorbents such as iron-containing solid wastes [7], sludge [8], carbonate-based magnetic materials [9], waste textile fiber [10] and agricultural wastes [11] for adsorption applications.

This study focused on preparation of chitosan/marble powder composite as a novel low cost adsorbent to determine its removal efficiency for Dimazol Red dye from aqueous solution. The dye adsorption process was carried out by batch experiments. The effective of contact time, pH, adsorbent dosage and initial dye concentration on adsorption process were determined. More important, adsorption isotherm and kinetic models were also discussed to analyze the interaction between dye molecules and adsorbent.

2. Materials and methods

2.1. Materials

The marble powder was collected from the local marble cutting/processing industry in Bilecik, Turkey. Chitosan (degree of deacetylation 75-85 %) was purchased from Aldrich. Aqueous acetic acid (Merck) solution was used as a solvent for the chitosan. Glutaraldehyde solution (50 %) was purchased from Fluka and used as a crosslinker.

[a] Corresponding author; caglayan.acikgoz@bilecik.edu.tr

Dimozol Red (purity of 99 %) was obtained from a dye factory in Bursa, Turkey. Adjusting the natural pH of the dye solution with HCl (0.1 M) or NaOH (0.1 M) solutions. All other chemicals were analytical grade and used without further purification.

2.2. Chitosan/marble powder composites

The method for the preparation of the Chitosan/marble powder composites were given in our previous study[12]. The summary of the method was given in the following description. 1 g of chitosan was dissolved in 75 mL of 5 % v/v acetic acid with constant stirring in order to get a homogeneous mixture. Marble powder was added and the mixture was left overnight with continuous stirring on magnetic stirrer resulting in the formation of the dispersion. The dispersion was taken in a syringe and allowed to fall slowly and dropwise into 1 M NaOH solution with gentle stirring, The composites were kept in the same solution overnight with continuous stirring. After the process, the chitosan/marble powder composites were washed many times with distilled water to attain a neutral pH. Glutaraldehyde was selected as a crosslinker, and the rinsed chitosan/marble powder was shaken in 2.5 w % glutaraldehyde ethyl alcohol solution. After 15 h crosslinking reaction at 60 °C, the chitosan/marble powder composite was rinsed with water again to remove excess glutaraldehyde and then freeze dried for 48 h. Finally, a series of chitosan/marble powder composites with different weight ratio percentage were synthesized, viz., 100:0 wt.% (C100M0), 70:30 wt.% (C70M30), 50:50 wt.% (C50M50), 30:70 wt.% (C30M70) .

2.3. Adsorption experiments

In order to evaluate the adsorption behaviour of the chitosan/marble powder composites, 0.1 g adsorbent was put into 50 mL Dimozol Red Dye solution with fixed concentrations (60 mg L-1).The mixtures were kept in a thermostat shaker (Termal H11960) with a shaking speed of 150 rpm at natural pH and room temperature for 72 h.

The concentrations of Dimozol Red in aqueous solution were determined using a UV–vis spectrophotometer (Agilent Cary 60 UV-Vis) at wavelength 540 nm. The adsorption capacities were calculated according to Equation (1):

$$q_e = \frac{(C_0 - C_e)V}{W} \quad (1)$$

where qe was the equilibrium adsorption capacity (mg/g), C0 and Ce were the initial and equilibrium concentrations (mg/L) of the dyes, respectively. V was the volume (L) of the solution and W was the weight (g) of the adsorbent.

3. Results and discussion

3.1. Effect of contact time and adsorption kinetics

Adsorptive uptake is one of the most significant term in adsorption process which determines the contact time. In generally, the least effective adsorption time is desired.Figure 1 presents the results of contact time on the adsorption of Dimozol Red dye onto chitosan/marble powder composites from waste water. The rate of adsorption of Dimozol Red was rapid in the beginning, proceeded at a slower rate and finally attained equilibrium at about 72 hours. At equilibrium, the adsorption capacity of Dimozol Red onto C100M0, C70M30 and C50M50 is about 28 mg/g and higher than that onto C30M70. Chitosan/marble powder composite with 50 %: 50 % weight percentage ratio of chitosan and marble powder, C50M50, was more economically than C100M0, C70M30 due to higher marble powder content and hence was selected as an adsorbent for all the other studies.

Dimozol Red onto different chitosan/marble powder composites (adsorbent dosage: 2 g/L, initial dye concentration: 60 mg/L, agitation speed: 150 rpm, temperature: 25°C).

The controlling mechanism of Dimozol Red dye adsorption on chitosan/marble powder composites was evaluated in terms of adsorption kinetics by measuring adsorption capacity at various time intervals till equilibrium value was reached. For kinetic study, the pseudo-first order model, the pseudo-second order model and the intra-particle diffusion model are used to evaluate the experimental data as the following three equations, respectively [13,14]:

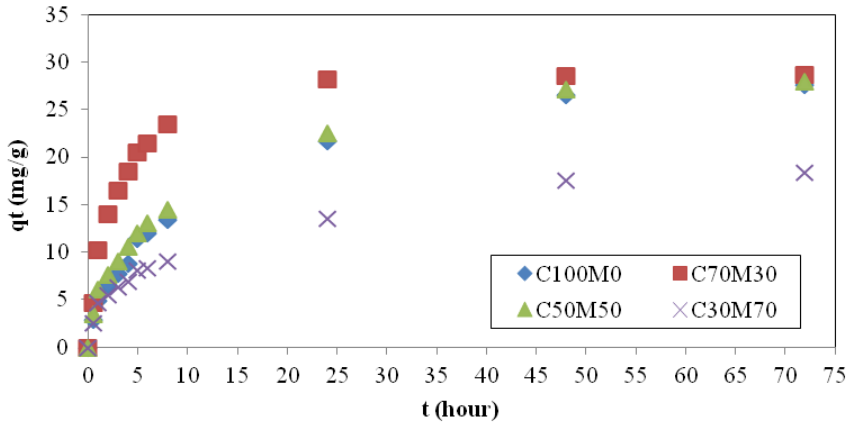

Figure 1. Effect of contact time on the adsorption of Dimozol Red onto different chitosan/marble powder composites (adsorbent dosage: 2 g/L, initial dye concentration: 60 mg/L, agitation speed: 150 rpm, temperature: 25°C).

$$\log(q_e - q_t) = \log q_e - \frac{k_1}{2.303} t \quad (2)$$

$$\frac{t}{q_t} = \frac{1}{k_2 q_e^2} + \frac{t}{q_e} \quad (3)$$

$$q_t = K_i \, . \, t^{1/2} + C \quad (4)$$

where qe (mg/g) and qt (mg/g) are the amount of the dyes adsorbed at equilibrium and at time t, respectively. The term k1 (hour−1) is the rate constant of pseudo-first order kinetic, and the term k2 (g/(mg·hour)) is the rate constant of pseudo-second order kinetic. Ki is the intra-particle diffusion rate constant (mg/g.hour-1/2), C is the constant for the experiment (mg/g).

The plots of linearized form of the pseudo-first-order, pseudo-second-order and the intra-particle diffusion equations are shown in Figure 2 (a), Figure 2 (b) and Figure 2 (c), respectively. Table 1 presents the characteristics parameters of the kinetic models. The R2 values (0.9851–0.9990) for pseudo-second-order kinetic model at all the composites (C100M0, C70M30, C50M50 and C30M70) are higher than those for pseudo-first order model. Also, the theoretical qe,cal values obtained from this model was closer and good agreement with the experimental values (qe,exp). It was suggested that the pseudo-second-order model is more suitable for describing the adsorption of Dimozol Red onto the chitosan/marble powder composite.

Table 1. Kinetic parameters for Dimozol Red dye adsorption on different chitosan/marble powder composites.

Adsorbents	Pseudo-first-order				Pseudo-second-order			intra-parcle diffusion	
	$q_{e,exp}$ (mg/g)	$q_{e,cal}$ (mg/g)	k_1(x10^3) (hour^{-1})	R^2	$q_{e,cal}$ (mg/g)	k_2(x10^3) (hour^{-1})	R^2	$k_{i,1}$ (mg/g.hour$^{-1/2}$)	$k_{i,2}$ (mg/g.hour$^{-1/2}$)
C100M0	27.61	30.65	100.87	0.9309	29.94	4.82	0.9851	4.8782	1.6972
C70M30	28.69	16.88	105.94	0.9740	29.59	17.41	0.9990	8.6846	0.1468
C50M50	28.00	25.85	79.22	0.9851	29.85	5.81	0.9889	5.1824	1.5593
C30M70	20.18	15.69	32.93	0.9718	19.42	9.01	0.9839	3.1905	1.3950

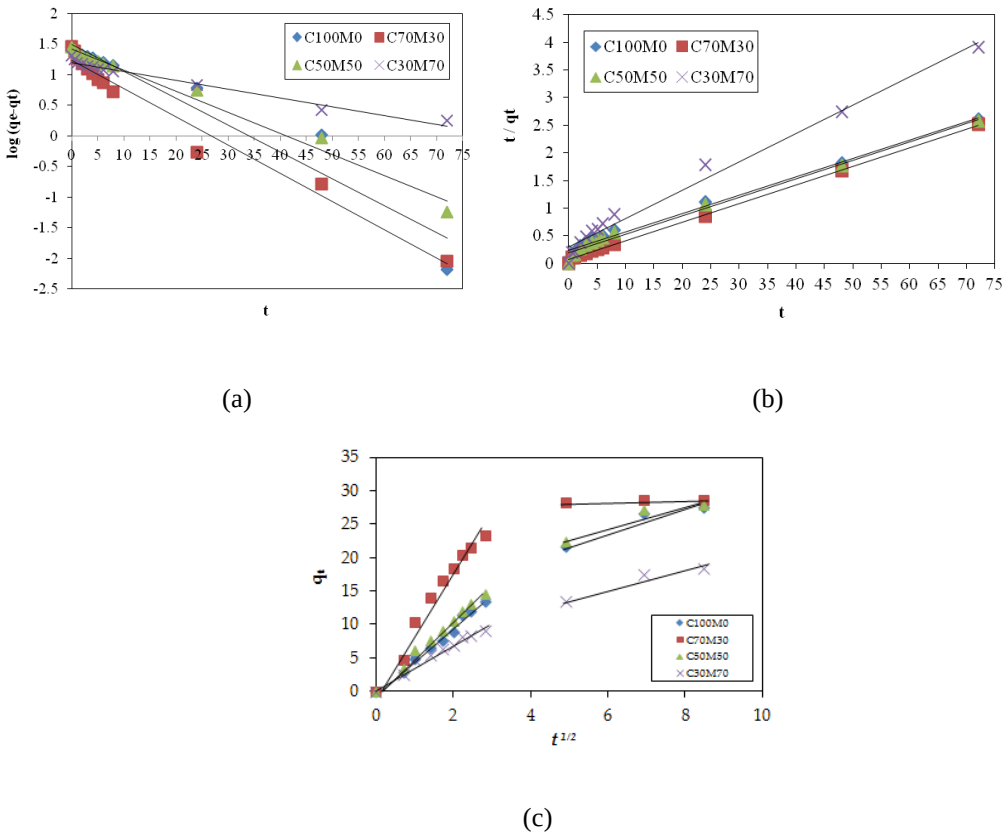

Figure 2. Kinetic models for the adsorption of Dimozol Red dye onto different chitosan/marble powder composites (a) Pseuso-first order, (b) Pseudo-second-order, (c) Intra-particle diffusion model.

To further explore the mechanisms of Dimozol Red dye adsorption on the chitosan/marble powder composites, the experimental data were analyzed by the intra-particle diffusion model. The transfer of the dye molecules from bulk liquid to active sites in the adsorbent could be controlled by mass transfer across the liquid film surrounding the solids (boundary layer diffusion) or mass transfer through pores (intra-particle diffusion), or a combination of both [14]. The first diffusion stage is the highly fast and the ki,1 rate constants for adsorption of Dimozol Red on the chitosan/marble powder composites are significantly higher than the ki,2, which might be attributed to the existence of fresh active sites on the chitosan/marble powder composites surface. When all of the exterior active sites of the chitosan/marble powder composites were occupied, Dimozol Red molecules seek to enter into the pores [15]. Then, the adsorption gradually slows down as shown by second linear portion of the curves (Figure 2 (c)).

3.2. Effect of initial solution pH and adsorbent dosage on dye adsorption

The adsorptive uptake of C50M50 composites to remove Dimozol Red was studied in a pH range of 3-11 at 298 K for 72 h. The effect of pH on the dye removal efficiency on the C50M50 composites was illustrated in Figure 3. The highest adsorption capacity of C50M50 composites was achieved at pH 5 and the lowest adsorption capacity at pH 11.

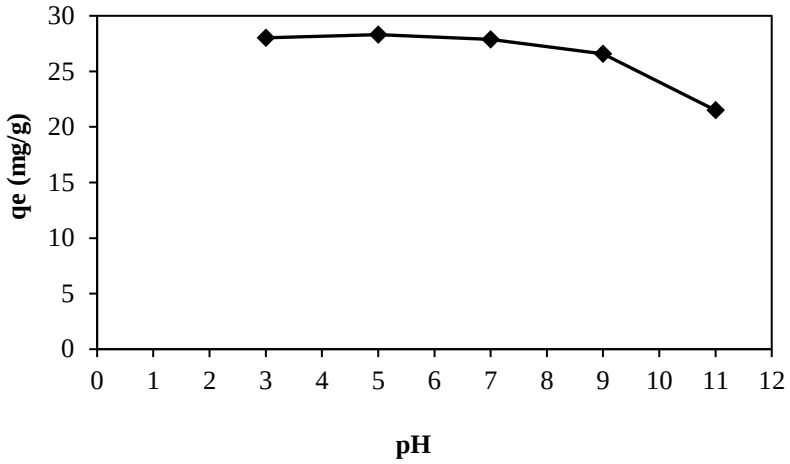

Figure 3. Effect of pH for the removal of Dimozol Red onto C50M50 composites.

The influence of adsorbent dosage was investigated by performing experiments at different adsorbent dosage from 0.2 to 2 g/L. In all experiments, 60 mg/L initial dye concentration and 25°C temperature was fixed as an optimum conditions. The results of adsorbent dosage effect on adsorption capacity were showed in Figure 4. The amount of dye adsorbed onto the C50M50 composites was found to decrease from 199.6 to 28.7 mg/g with increasing adsorbent dose due to the concentration gradient between adsorbent and adsorptive [16].

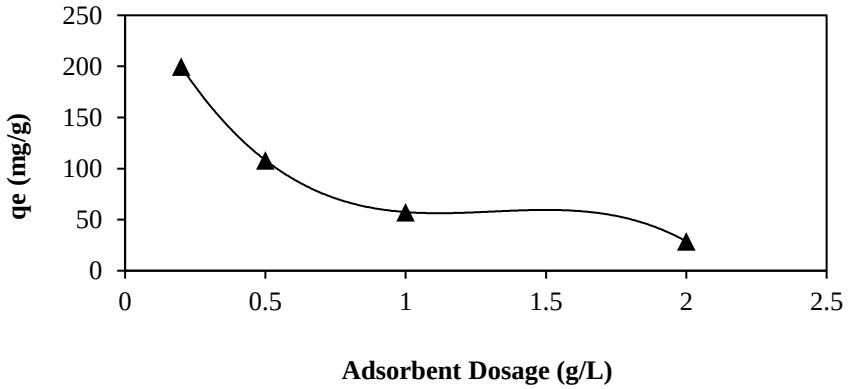

Figure 4. Effect of adsorbent dosage on the adsorption capacity of C50M50 composites.

3.4. Adsorption isotherms

Langmuir, Freundlich, Temkin and Dublin-Radushkevich adsorption isotherm models were used to design and to understand the mechanism of interaction existing between adsorbate and the adsorbent at equilibrium.

Equilibrium data for Dimozol Red adsorption on the C50M50 composites were applied to Langmuir, Freundlich, Temkin and Dublin-Radushkevich equations [17-20]:

Langmuir Isotherm:

$$C_e/q_e = C_e/q_m + 1/(q_m . K_L) \quad (5)$$

where Ce (mg/L) is the equilibrium concentration, qe (mg/g) is the equilibrium adsorption capacity, qm (mg/g) is the maximum adsorption capacity at monolayer coverage, KL (L/mg) is the Langmuir isotherm constant related to free energy of adsorption.

Freundlich Isotherm:

$$\ln q_e = \ln K_F + (1/n) . (\ln C_e) \quad (6)$$

where KF [mg/g (L/g)1/n] is the Freundlich adsorption constant related to the adsorption capacity, n is the Freundlich constant related to the affinity of the adsorbate to the adsorbent.

Temkin Isotherm:

$$q_e = B \ln A_T + B \ln C_e \quad (7)$$

where A (mg/L) is the Temkin isotherm equilibrium constant related to binding energy, and B (RT/bT) is the Temkin constant related to the adsorption heat.

Dublin-Radushkevich Isotherm:

$$\ln q_e = -\beta . \varepsilon^2 + \ln q_{m,D-R} \quad (8)$$

where β (mol2/kJ) is a constant related to mean sorption energy, qm,D-R (mg/g) is the theoretical adsorption capacity, Ɛ is the Polanyi potential (kJ/mol) calculated based on Equation 9:

$$\varepsilon = R.T.\ln\left(\frac{C_e+1}{C_e}\right) \quad (9)$$

The adsorption mean free energy, E (kJ/mol), was calculated from D-R isotherm using Equation 10:

$$E = \frac{1}{\sqrt{2\beta}} \quad (10)$$

Figure 5 shows the plot of ln qe vs. ln Ce for the Freundlich model, the plot of Ce/qe vs. Ce for the Langmuir model, the plot of ln Ce vs. qe for the Temkin model and the plot of Ɛ2 vs. ln qe for the Dublin-Radushkevich model. The applicability of the four isotherm's model for the present data approximately follows the order: Freundlich, Langmuir, Temkin and Dublin-Radushkevich. The coefficient of determination R2 (0.9814) for the Freundlich model is higher than that of the other models. Based on R2 value, the Freundlich model is more suitable in describing the experimental data for Dimozol Red adsorption onto C50M50 composites. The values of Kf and n calculated from the intercept and slope of the linearized Freundlich model are listed in Table 2. The value of 1/n is lower than 1.0, which indicates the heterogeneity of the adsorption process and also to be favorable.

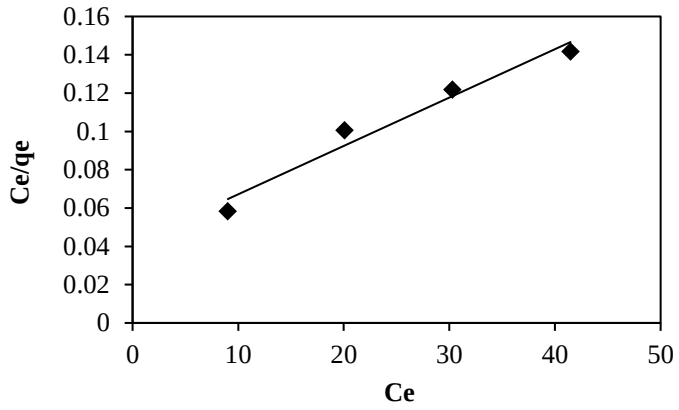

(a)

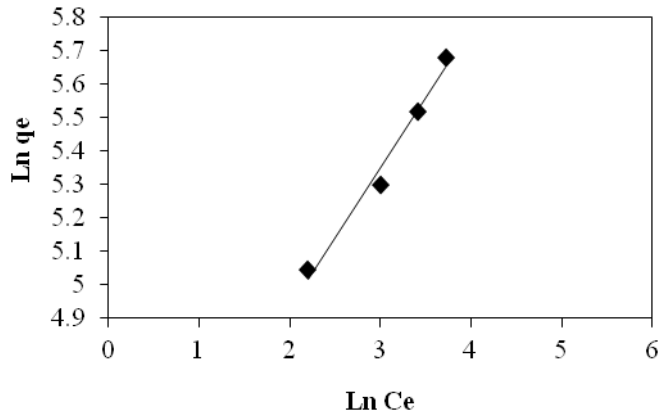

(b)

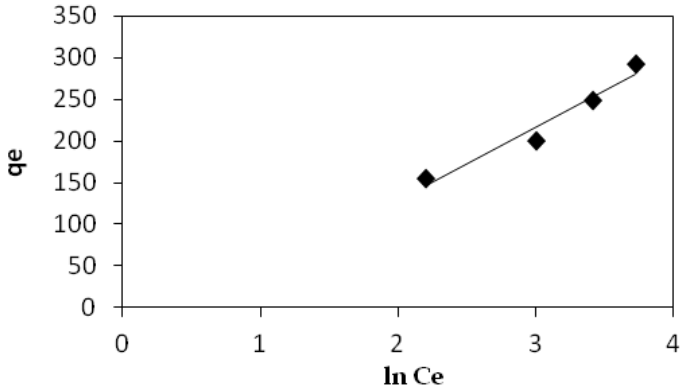

(c)

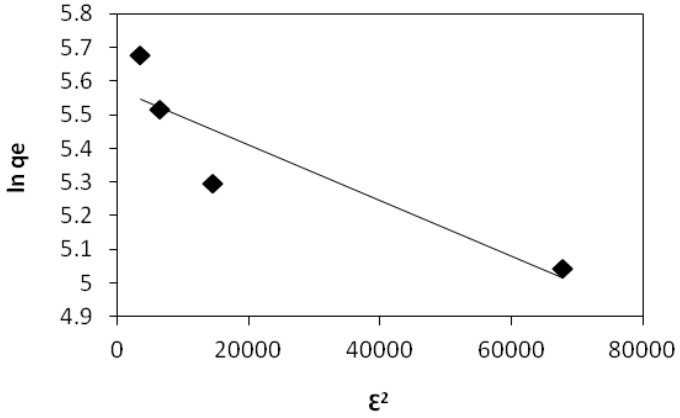

(d)

Figure 5. Isotherm models for Dimozol Red dye adsorption by C50M50 composites (a) Langmuir, (b) Freundlich, Temkin (c) and Dublin-Radushkevich (d) (adsorbent dosage: 0.2 g/L, initial dye concentration: 40 -100 mg/L, agitation speed: 150 rpm, temperature: 25°C).

Table 2. Adsorption isotherm parameters for the adsorption of Dimozol Red onto C50M50 composites.

Isotherms	**Parameters**	
Langmuir	q_m	400
	K_L	0.0597
	R^2	0.9633
Freundlich	n	2.4137
	K_F	60.69
	R^2	0.9814
Temkin	A_T	0.5803
	B	88.184
	b_T	28.08
	R^2	0.9505
Dublin-Radushkevich	$q_{m,D-R}$	263,3
	E	0,246
	R^2	0.8093

4. Conclusions

In this study, chitosan and marble powder was used to synthesize chitosan/marble powder composites as novel and cost-effective adsorbent. The composite was used to adsorp Dimozol Red anionic dye from

aqueous solution. Furthermore, the influence of several parameters such as contact time, pH, adsorbent dosage and initial dye concentration was investigated. Under the optimal conditions (pH:5; 100 mg/L initial dye concentration, adsorbent dosage: 0.01g), the experimental maximum adsorption capacity was achieved as 292.7 mg/g. Isotherm studies suggested that the experimental data was well fitted to the Freundlich model at all concentration values. Adsorption kinetic data was well fitted by pseudo-second-order kinetic model. The results show that the synthesized novel chitosan/marble powder composites are an efficient and low cost adsorbent for removal of Dimozol Red from aqueous solution and is a promising adsorbent for removing dyes from textile and other wastewater.

References

[1] Bilal, M., Iqbal, H. M., Hu, H., Wang, W., Zhang, X. Enhanced bio-catalytic performance and dye degradation potential of chitosan-encapsulated horseradish peroxidase in a packed bed reactor system. Science of the Total Environment 2017; 575; 1352-1360, 10.1016/j.scitotenv.2016.09.215.

[2] Bassyouni, D. G., Hamad, H. A., El-Ashtoukhy, E. Z., Amin, N. K., El-Latif, M. A. Comparative performance of anodic oxidation and electrocoagulation as clean processes for electrocatalytic degradation of diazo dye Acid Brown 14 in aqueous medium. Journal of Hazardous Materials 2017; 335: 178-187, 10.1016/j.jhazmat.2017.04.045.

[3] Bazrafshan, E., Alipour, M. R., Mahvi, A. H. Textile wastewater treatment by application of combined chemical coagulation, electrocoagulation, and adsorption processes. Desalination and Water Treatment 2016; 57(20): 9203-9215, 10.1080/19443994.2015.1027960

[4] Guin, J. P., Bhardwaj, Y. K., Varshney, L. Mineralization and biodegradability enhancement of Methyl Orange dye by an effective advanced oxidation process. Applied Radiation and Isotopes 2017; 122: 153-157, doi.org/10.1016/j.apradiso.2017.01.018.

[5] Lipatova, I. M., Makarova, L. I., Yusova, A. A. Adsorption removal of anionic dyes from aqueous solutions by chitosan nanoparticles deposited on the fibrous carrier. Chemosphere 2018; 212: 1155-1162, doi.org/10.1016/j.chemosphere.2018.08.158.

[6] Vakili, M., Rafatullah, M., Salamatinia, B., Abdullah, A.Z., Ibrahim, M.H., Tan, K.B. Application of chitosan and its derivatives as adsorbents for dye removal from water and wastewater: A review. Carbohydrate polymers 2014; 113: 115-130, 10.1016/j.carbpol.2014.07.007.

[7] Iakovleva, E., Maydannik, P., Ivanova, T.V., Sillanpää, M., Tang, W.Z., Mäkilä, E. Modified and unmodified low-cost iron-containing solid wastes as adsorbents for efficient removal of As (III) and As (V) from mine water. Journal of Cleaner Production 2016; 133: 1095-1104, 10.1016/j.jclepro.2016.05.147.

[8] Xu, G., Yang, X., Spinosa, L. Development of sludge-based adsorbents: Preparation, characterization, utilization and its feasibility assessment. Journal of environmental management 2015; 151: 221-232, 10.1016/j.jenvman.2014.08.001.

[9] Islam, M.S., San Choi, W., Nam, B., Yoon, C., Lee, H.J. Needle-like iron oxide@CaCO3 adsorbents for ultrafast removal of anionic and cationic heavy metal ions. Chemical Engineering Journal 2017; 307: 208-219, 10.1016/j.cej.2016.08.079.

[10] Bediako, J.K.., Wei, W., Yun, Y.S. Conversion of waste textile cellulose fibers into heavy metal adsorbents. Journal of Industrial and Engineering Chemistry 2016; 43: 61-68, 10.1016/j.jiec.2016.07.048.

[11] de Luna, M.D.G., Budianta, W., Rivera, K.K.P., Arazo, R.O. Removal of sodium diclofenac from aqueous solution by adsorbents derived from cocoa pod husks. Journal of Environmental Chemical Engineering 2017; 5: 1465-1474, 10.1016/j.jece.2017.02.018.

[12] Akin Sahbaz, D., Acikgoz, C. Cross- Linked Chıtosan/Marble Powder Composites for The Adsorptıon of Dimozol Blue. Water Science and Technology 2017; 76(9-10): 2776-2784. doi: 10.2166/wst.2017.447.

[13] Hajati, S., Ghaedi, M., Karimi, F., Barazesh, B., Sahraei, R., Daneshfar, A. Competitive adsorption of Direct Yellow 12 and Reactive Orange 12 on ZnS: Mn nanoparticles loaded on activated carbon as novel adsorbent. Journal of Industrial and Engineering Chemistry 2014; 20(2): 564-571, 10.1016/j.jiec.2013.05.015.

[14] Weber, W. J., Morris, J. C. Kinetics of adsorption on carbon from solution. Journal of the Sanitary Engineering Division 1963; 89(2):

31-60. 15.
[15] Tanhaei, B., Ayati, A., Lahtinen, M., Sillanpää, M. Preparation and characterization of a novel chitosan/Al2O3/magnetite nanoparticles composite adsorbent for kinetic, thermodynamic and isotherm studies of Methyl Orange adsorption. Chemical Engineering Journal 2015; 259: 1-10, 1-10.doi.org/10.1016/j.cej.2014.07.109.
[16] Zhu, H.Y., Jiang, R., Xiao, L. Adsorption of an anionic azo dye by chitosan/kaolin/γ-Fe2O3 composites. Applied Clay Science 2010; 48(3): 522-526, 10.1016/j.clay.2010.02.003.
[17] Wibowo, E., Rokhmat, M., Abdullah, M. Reduction of seawater salinity by natural zeolite (Clinoptilolite): Adsorption isotherms, thermodynamics and kinetics. Desalination 2017; 409: 146-156, 10.1016/j.desal.2017.01.026.
[18] De Castro, M. L. F. A., Abad, M. L. B., Sumalinog, D. A. G., Abarca, R. R. M., Paoprasert, P., de Luna, M. D. G. Adsorption of Methylene Blue dye and Cu (II) ions on EDTA-modified bentonite: Isotherm, kinetic and thermodynamic studies. Sustainable Environment Research 2018; 28: 197-205, 10.1016/j.serj.2018.04.001.
[19] Wang, X., Jiang, C., Hou, B., Wang, Y., Hao, C., Wu, J. Carbon composite lignin-based adsorbents for the adsorption of dyes. Chemosphere 2018; 206: 587-596, 10.1016/j.chemosphere.2018.04.183.
[20] Liu, M., Hou, L. A., Xi, B., Zhao, Y., Xia, X. Synthesis, characterization, and mercury adsorption properties of hybrid mesoporous aluminosilicate sieve prepared with fly ash. Applied Surface Science 2013; 273: 706-716, 10.1016/j.apsusc.2013.02.116.